JOURNAL OF PROPULSION AND POWER
Vol. 11, No. 5, September–October 1995

Mixing Analysis of Axially Opposed Rows of Jets Injected into Confined Crossflow

D. B. Bain* and C. E. Smith†
CFD Research Corporation, Huntsville, Alabama 35805
and
J. D. Holdeman‡
NASA Lewis Research Center, Cleveland, Ohio 44135

A CFD parametric study was performed to analyze axially opposed rows of jets mixing with crossflow in a rectangular duct. Isothermal analysis was conducted to determine the influence of lateral geometric arrangement on mixing. Two lateral arrangements were analyzed: 1) inline (jets' centerlines aligned with each other on top and bottom walls) and 2) staggered (jets' centerlines offset with each other on top and bottom walls). For a jet-to-mainstream mass-flow ratio (*MR*) of 2.0, design parameters were systematically varied for jet-to-mainstream momentum-flux ratios *J* between 16–64, and orifice spacing-to-duct height ratios *S/H* between 0.125–1.5. Comparisons were made between geometries optimized for *S/H* at a specified *J*. Inline configurations had a unique spacing for best mixing at a specified *J*. In contrast, staggered configurations had two "good mixing" spacings for each *J*, one corresponding to optimum inline spacing and the other corresponding to optimum wall-impinging jet spacing. The inline configurations, due to their smaller orifice size at optimum *S/H*, produced better initial mixing characteristics. At downstream locations (e.g., axial distance-to-duct height ratio of 1.5), the optimum staggered configuration produced better mixing than the optimum inline configuration for *J* of 64; the opposite results were observed for *J* of 16. Increasing *J* resulted in better mixing characteristics if each configuration was optimized with respect to orifice spacing. For jet-to-mainstream *MR*s of 2.0, the optimum mixing equation [$(S/H)\sqrt{J} = C$] of Holdeman was substantiated, except the optimum mixing constant *C* increased by a factor of 1.8 for two-sided inline configurations.

Nomenclature

C	=	$(S/H)\sqrt{J}$, see Eq. (1)
C_{avg}	=	$m_j/(m_j + m_\infty) = \theta_{EB}$
H	=	duct height
J	=	momentum-flux ratio $(\rho_j V_j^2)/(\rho_\infty U_\infty^2)$
L	=	orifice length (long dimension)
L/W	=	orifice AR
MR	=	mass-flow ratio, m_j/m_∞
m_j	=	mass flow of jets
m_∞	=	mass flow of mainstream flow
P	=	pressure, N/m^2
S	=	orifice spacing
S/H	=	orifice spacing-to-duct height ratio
T	=	temperature, K
U	=	unmixedness, see Eq. (2)
U_∞	=	mainstream flow velocity, m/s
u	=	rms of axial velocity fluctuation
V_j	=	jet velocity, m/s
v	=	rms of vertical velocity fluctuation
W	=	orifice width (short dimension)
x	=	axial coordinate, $x = 0$ at leading edge of the orifice
x/H	=	axial distance-to-duct height ratio
y	=	vertical coordinate
z	=	lateral coordinate
μ_T	=	turbulent viscosity, kg/m·s
ρ_j	=	density of jet
ρ_∞	=	density of mainstream

Received Dec. 8, 1993; revision received Oct. 9, 1994; accepted for publication Oct. 23, 1994.

*Project Engineer, 3325 Triana Blvd. Member AIAA.
†Vice President/Engineering, 3325 Triana Blvd. Member AIAA.
‡Senior Research Engineer, Internal Fluid Mechanics Division. Associate Fellow AIAA.

I. Introduction

THE technology demonstration of low NO_x combustors applicable to commercial aircraft is a subject of ongoing research.[1] One combustor concept currently being evaluated both numerically and experimentally is the rich-burn/quick-mix/lean-burn (RQL) combustor. The RQL combustor utilizes staged burning.[2] In this concept, the rich-burn zone is designed to operate at equivalence ratios greater than 1. The combustion products from the rich-burn section enter the quick-mix section where mixing takes place with bypass air. The combustion process is then completed in the lean-burn region.

A key design technology required for successful demonstration of the RQL concept is a method of rapidly mixing bypass air with rich-burn gases to suppress the formation of harmful emissions. Recent studies have been performed that focus on identifying improved mixing concepts.[3–13] The current investigation focuses on jet mixing in rectangular cross-sectional ducts.

II. Background

The mixing of jets in a confined crossflow has been important in gas turbine combustion applications for many years. Perhaps foremost in importance is the jet mixing that occurs in the combustor dilution zone. In conventional annular gas turbine combustors, the dilution zone is the aft zone in which air dilutes combustion products before entering the turbine. The dilution jets should effectively penetrate and mix with combustion gases, thereby establishing a temperature profile acceptable to the turbine. The typical range of jet-to-mainstream mass-flow ratio (MR) is 0.25–0.50.

RQL jet mixing applications offer some sharp contrasts to conventional dilution zone mixing. First, the mass-flow ratio is approximately 2.0. Such a large MR results in larger orifices, potentially creating jet blockage effects that can substantially affect mixing. Because round orifices may not be practical

Table 1 Numerical cases analyzed

Parametric	Case	Configuration	Slot AR	J	MR	S/H	Trailing edge, x/H	Jet blockage at wall, %
Parametric 1	1	Inline	4:1	36	2.0	0.125	0.29	57.7
	2					0.20	0.36	45.6
	3					0.228	0.39	42.8
	4					0.25	0.41	40.8
	5					0.275	0.43	38.9
	6					0.325	0.47	35.8
	7					**0.375**	**0.50**	**33.3**
	8					0.425	0.53	31.3
	9					0.50	0.58	28.9
	10					0.75	0.71	23.6
	11					0.85	0.75	22.1
Parametric 2	12	Staggered	4:1	36	2.0	0.375	0.50	33.3
	13					0.75	0.71	23.6
	14					**0.85**	**0.75**	**22.1**
	15					1.0	0.81	20.4
	16					1.25	0.91	18.3
	17					1.50	1.00	16.7
Parametric 3	18	Inline	4:1	16	2.0	0.325	0.57	43.8
	19					0.375	0.61	40.8
	20					0.425	0.65	38.4
	21					**0.50**	**0.70**	**35.4**
	22					0.55	0.74	33.7
	23					0.60	0.77	32.3
	24					1.00	1.00	25.0
Parametric 4	25	Staggered	4:1	16	2.0	0.50	0.70	35.4
	26					0.85	0.92	27.1
	27					**1.0**	**1.0**	**25.0**
	28					1.25	1.12	22.4
	29					1.30	1.14	21.9
	30					1.50	1.22	20.4
Parametric 5	31	Inline	4:1	64	2.0	0.125	0.25	50.0
	32					0.20	0.32	39.5
	33					0.25	0.35	35.4
	34					0.275	0.37	33.7
	35					**0.285**	**0.38**	**33.1**
	36					0.30	0.39	32.3
	37					0.325	0.40	31.0
	38					0.85	0.65	19.2
Parametric 6	39	Staggered	4:1	64	2.0	0.285	0.38	33.1
	40					0.50	0.50	25.0
	41					0.65	0.57	21.9
	42					0.75	0.61	20.4
	43					**0.85**	**0.65**	**19.2**
	44					1.00	0.71	17.7

Bold font represents optimum mixing configuration.

due to blockage and structural concerns, slots may be needed. Second, low pollutant levels are the drivers for "good" mixing in RQL applications, in contrast to temperature profile and "hot spots" for dilution zone applications.

Significant research has been performed for dilution zone mixing.[14] This research has identified two design variables that control jet penetration and mixing characteristics: 1) jet-to-mainstream momentum-flux ratio J and 2) orifice spacing-to-duct height ratio S/H. Single-sided (from one wall only) injection was extensively studied, while two-sided (from top and bottom walls) injection was studied to a lesser extent. Optimum mixing relationships were determined to be a function of $(S/H)\sqrt{J}$ for the range of conditions tested and analyzed:

$$C = (S/H)\sqrt{J} \tag{1}$$

For one-sided injection, optimum mixing was obtained when C was about 2.5.

Two-sided injection with an inline lateral arrangement was shown to be similar to one-sided injection if the duct was considered sliced in half, yielding a constant of proportionality

Table 2 Mainstream and jet flow conditions

Mainstream	Jets
U_∞ = 10 m/s	V_j = 40 m/s[a]
	60 m/s
	80 m/s
T_∞ = 300 K	T_j = 300 K
u/U_∞ = 0.20	v/V_j = 0.20
$\mu_T = 1 \times 10^{-2}$ kg/m·s	$\mu_T = 1 \times 10^{-2}$ kg/m·s
$P = 1 \times 10^5$ N/m^2	
J = 16, 36, 64	
m_j/m_∞ = 2.0	

[a] V_j varies according to specified J.

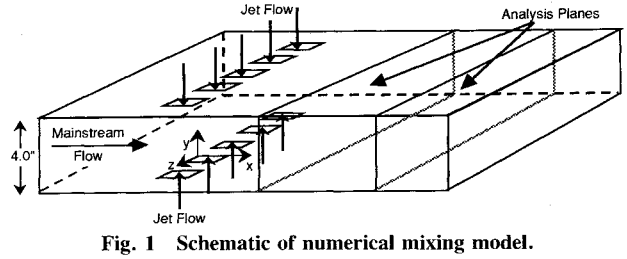

Fig. 1 Schematic of numerical mixing model.

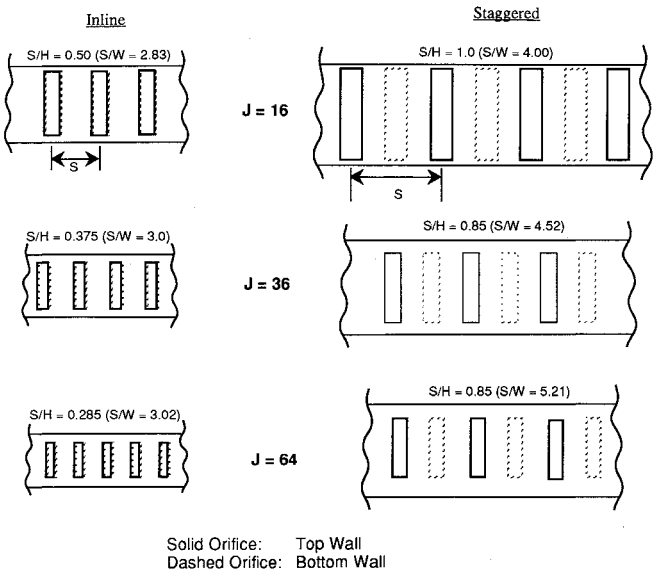

Fig. 2 Slot configurations at optimum *S/H*.

that is one-half of the corresponding value for one-sided injection. Thus, a C of 1.25 would be expected for optimum mixing of opposed rows of jets with centerlines inline.

For two-sided injection with a staggered lateral arrangement, very little data, either experimentally or numerically, have been generated. Holdeman[14] has suggested staggered holes produce optimum mixing if the jets penetrate past each other. He determined (from the few tests conducted) that best mixing was obtained when alternate jets for optimum one-sided injection were moved to the opposite wall. Thus, the correlation constant would be expected to be 5.0 for opposed rows of jets with centerlines staggered.

A basic question often arises concerning which lateral arrangement produces superior mixing: inline or staggered. This fundamental question has never truly been answered. Indeed, even combustor designers differ in their opinion, as evidenced by conventional dilution zones with both types of lateral alignments. As an added complication in this RQL application, past results may not be directly applicable due to the mass-flow ratio (0.50 for conventional dilution zone vs 2.0 for RQL). This study sought to address the lateral arrangement issue by a systematic computational investigation. A complete description of the cases studied and their results are discussed next.

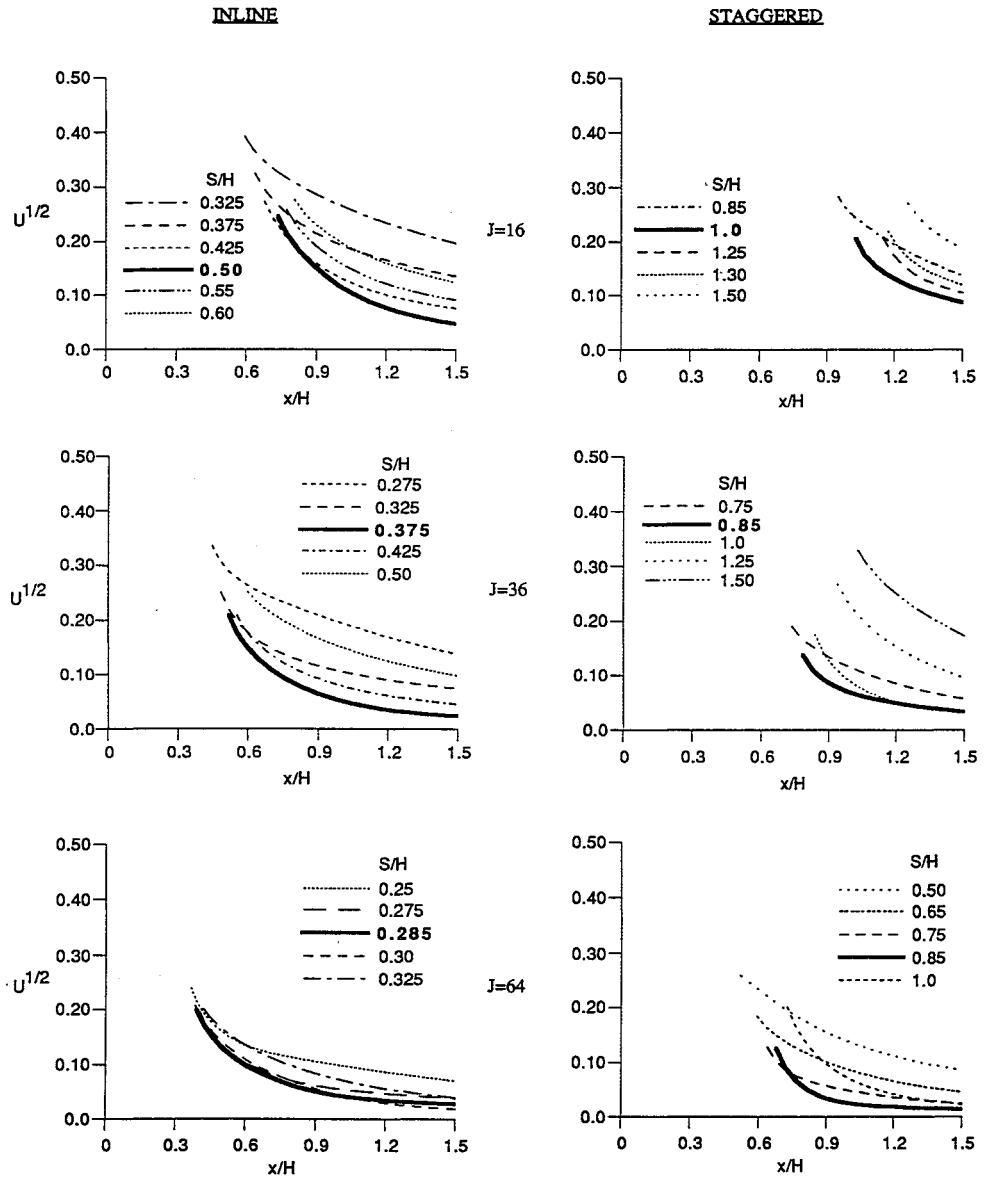

Fig. 3 Computational results of parametrics 1–6.

III. Computational Fluid Dynamics Code

The approach in this study was to perform three-dimensional numerical calculations on a generic geometry section. The CFD code named REFLEQS[15] was used to perform the computations. The basic capabilities/methodologies in REFLEQS include 1) solution of two- and three-dimensional, time-accurate or steady-state Navier–Stokes equations for incompressible and compressible flows; 2) Cartesian, polar, and nonorthogonal body-fitted coordinates; 3) porosity-resistivity techniques for flows with internal blockages; 4) fully implicit and strongly conservative formulation; 5) three differencing schemes: upwind, hybrid, and central differencing with damping terms; 6) standard, extended, and low Reynolds number k-ε turbulence models, and the multiple-scale turbulence model of Chen; 7) instantaneous, one-step and two-step combustion models; 8) modified form of Stone's strongly implicit solver; and 9) pressure-based solution algorithms including SIMPLE and a variant of SIMPLEC.

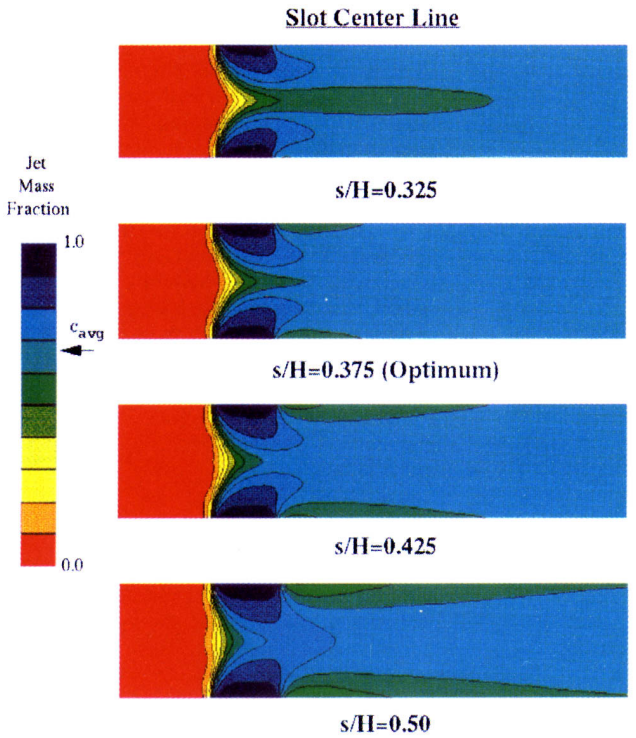

Fig. 4 Effect of jet penetration on mixing for inline slots: momentum-flux ratio 36, mass-flow ratio 2.0.

IV. Details of Numerical Calculations

A schematic diagram of the numerical model is shown in Fig. 1. The height of the mixing section was 4 in. (0.1016 m). The mainstream flow entered the calculation domain one duct height upstream (x/H of 1.0) of the leading edge of the orifices, and continued downstream to x/H of 7.0. The model consisted of jet injection from top and bottom walls into mainstream flow. All of the orifices were straight slots with an AR of 4:1, with the long dimension of the slot in the direction of the mainstream flow.

Two orifice arrangements were modeled: 1) staggered and 2) inline. For the staggered cases, the lateral calculation domain extended from midplane to midplane between top and bottom jet centerlines, and modeled one jet on the top wall and one jet on the bottom wall. Periodic boundary conditions were imposed along the lateral boundaries. For the inline cases, the lateral domain extended from midplane-to-midplane between the jets' centerlines. Again, periodic lateral boundary conditions were imposed. It should be noted that the staggered configurations consisted of twice the lateral domain of the inline configurations.

The boundary conditions at the mainstream and jet inlet planes were assumed to have a uniform velocity profile. The static pressure at the duct outlet plane was specified to be a constant value. In practical combustor analysis, the assumption of uniform velocity profiles is not necessarily valid and other flow effects could be present (i.e., elliptical effects in jet supply). For this generic analysis the inclusion of nonuniform jet velocity profiles or the inclusion of jet supply plenums was felt to be beyond the scope of this mixing study.

Six parametrics consisting of 44 cases were analyzed as shown in Table 1. The case sequence for each parametric

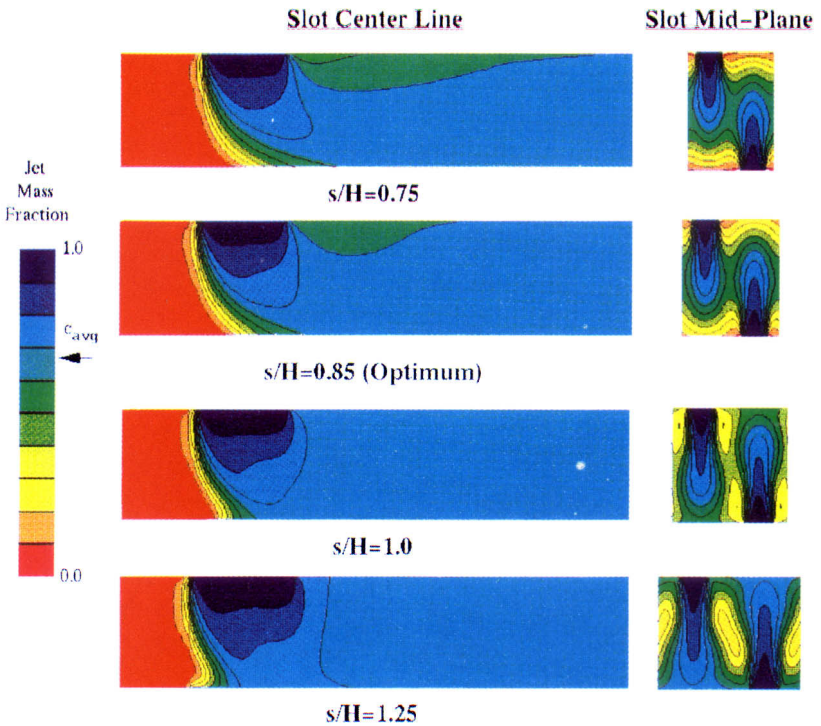

Fig. 5 Effect of jet penetration on mixing for staggered slots: momentum-flux ratio 36, mass-flow ratio 2.0.

consisted of fixing J (at 16, 36, or 64) and lateral arrangement (inline or staggered), and then parametrically changing S/H to optimize mixing. For each parametric, the slot geometry producing optimum mixedness is shown in Fig. 2.

The flow conditions of the mainstream and jets are shown in Table 2. The turbulent length scales of the jets were varied to maintain a constant inlet turbulent viscosity.

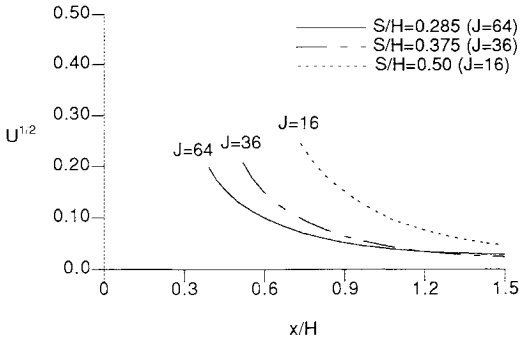

Fig. 6 Effect of J on unmixedness for inline slots: mass-flow ratio of 2.0.

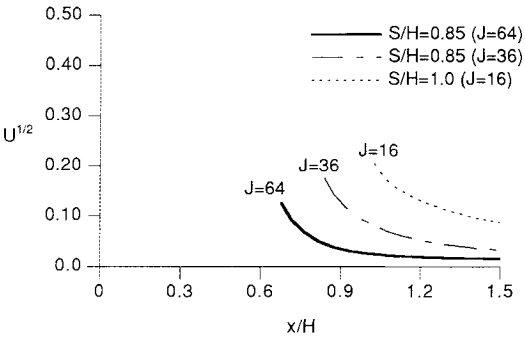

Fig. 7 Effect of J on unmixedness for staggered slots: mass-flow ratio of 2.0.

A. Grids

A typical staggered case consisted of 80,000 cells, 64 cells in the axial x direction, 28 cells in the vertical y direction, and 44 cells in the lateral z direction. The slots were composed of 144 (24 × 6) evenly distributed cells. The grid upstream and downstream of the slot region was expanded/contracted so that each cell adjacent to the slot region matched the cell size in the slot region. The cells in the vertical direction were all of uniform size. Note that the grid size for the inline cases was typically half the size for the staggered cases.

In earlier works,[8] a much finer grid (≈145,000 cells) was used in the numerical calculations. Since that paper, a grid density study has been performed and it was determined that such fine grids are not needed for engineering calculations. Thus, the number of cells was reduced for computational efficiency in this study.

B. Numerics

The following conservation equations were solved: u momentum, v momentum, w momentum, mass (pressure correction), turbulent kinetic energy k, turbulent energy dissipation ε, and composition mixture fraction f. The convective fluxes were calculated using upwind differencing, and the diffusive fluxes were calculated using central differencing. The standard k-ε turbulence model was employed and conventional wall functions were used. A turbulent Sc of 0.9 was assumed and held constant.

C. Convergence

All error residuals were reduced at least six orders of magnitude, and continuity was conserved in each axial plane to the fifth decimal. Convergence was relatively smooth, requiring about 600 iterations. A converged solution required approximately 4.0 CPU hours on a Cray Y-MP computer.

V. Data Postprocessing

In order to quantify the mixing effectiveness, the area-averaged spatial concentration variance of jet flow was calculated in each axial plane. The use of area-averaged quantities, rather than mass flowaveraged quantities, was chosen to be consistent with concurrent experimental measurements

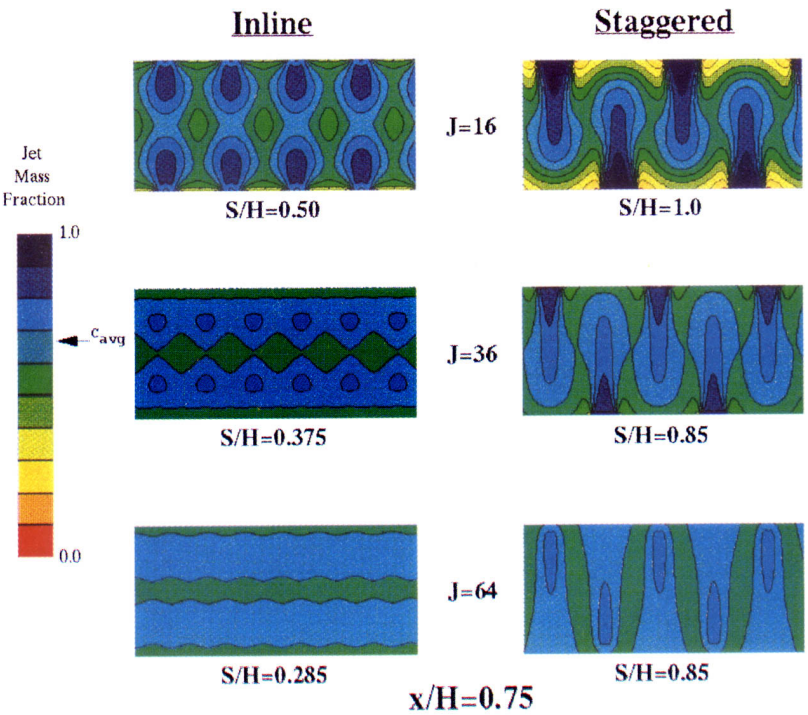

Fig. 8 Effect of J variation on mixing for inline and staggered slots: mass-flow ratio 2.0.

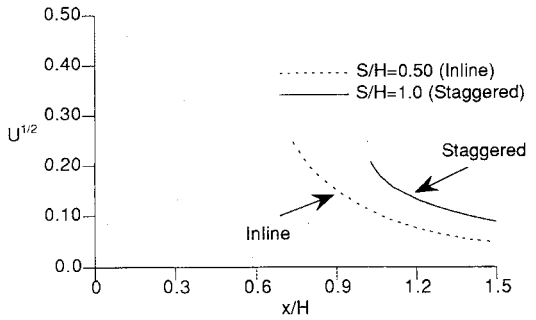

Fig. 9 Effect of lateral arrangement on unmixedness, J = 16.

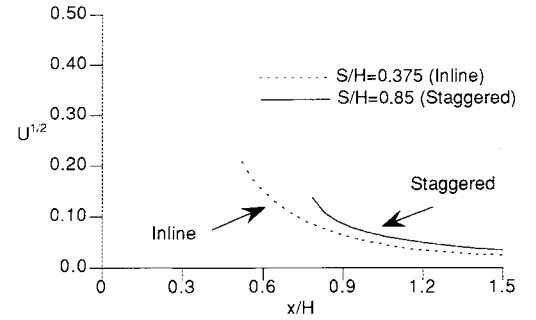

Fig. 10 Effect of lateral arrangement on unmixedness, J = 36.

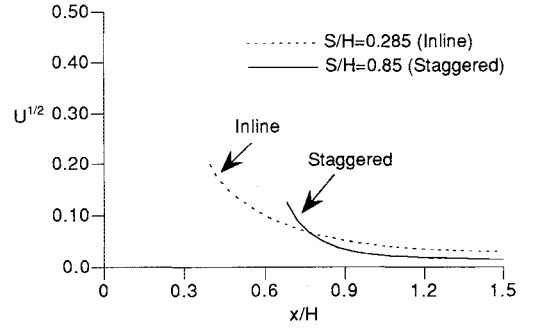

Fig. 11 Effect of lateral arrangement on unmixedness, J = 64.

and allow one-to-one comparison. The area-averaged unmixedness U is defined[16] as

$$U = C_{var}/[C_{avg}(1 - C_{avg})] \quad (2)$$

where

C_{var} = $(1/A_{TOT})\ \Sigma_i\ A_i(C_i - C_{avg})^2$
A_{TOT} = total flow area in each axial plane
A_i = flow area of cell i
C_i = jet mass fraction in cell i

For this study, C_{avg} is 0.667.

The use of C_{avg} in determining U is only correct downstream of the slots' trailing edge. Upstream of the slots' trailing edge, the injection of jet mass-flow makes the use of C_{avg} incorrect. Therefore, the unmixedness values shown plotted in this article always begin one computational cell aft of the slots' trailing edge.

VI. Results and Discussion

Figure 3 displays the results for the inline and staggered configurations for a J of 16, 36, and 64. The optimum S/H ratio for each parametric is identified by the boldest curve. Discussion of these results is presented later.

A. Effect of S/H on Jet Penetration

A qualitative view of how S/H affects jet penetration and corresponding mixing levels is shown in Fig. 4. This figure shows the jet mass fraction concentrations for inline slots at J of 36. The views presented are lateral slices taken through the slot centerline. S/H variations are presented to illustrate the effect of S/H on jet penetration. At the smaller S/H, the jets are underpenetrated, allowing the approach flow to pass through the center of the duct. As S/H increases, the jets penetrate farther into the duct, beginning to pinch off the approach flow along the duct centerline. At the largest S/H the jets have clearly overpenetrated, blocking off most of the approach flow in the center of the duct and forcing more of the approach flow to go between the jets. S/H of 0.375 gives the optimum penetration that agrees well with the optimum S/H in terms of unmixedness (as shown in Fig. 3). In general

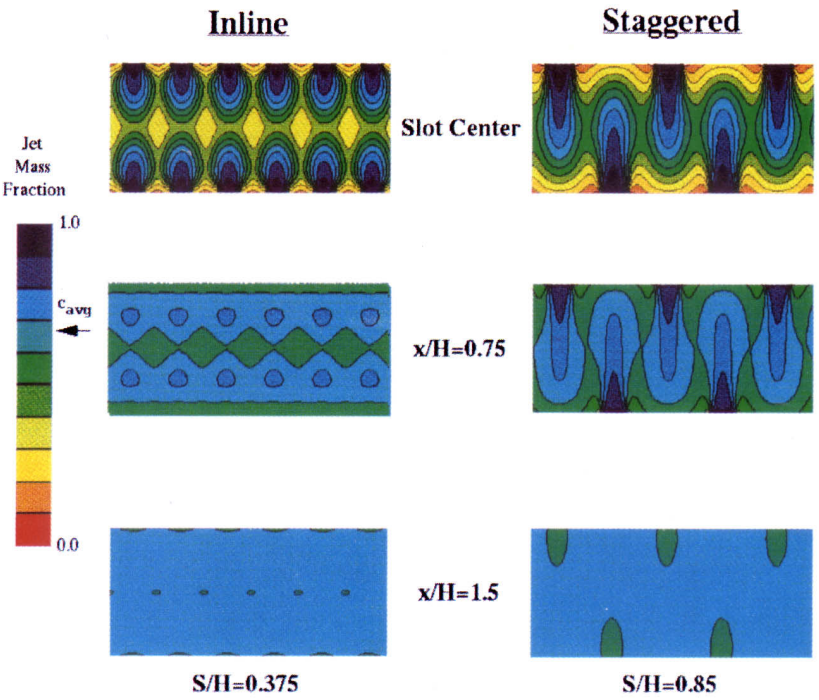

Fig. 12 Effect of lateral arrangement on mixing: J = 36, MR = 2.0.

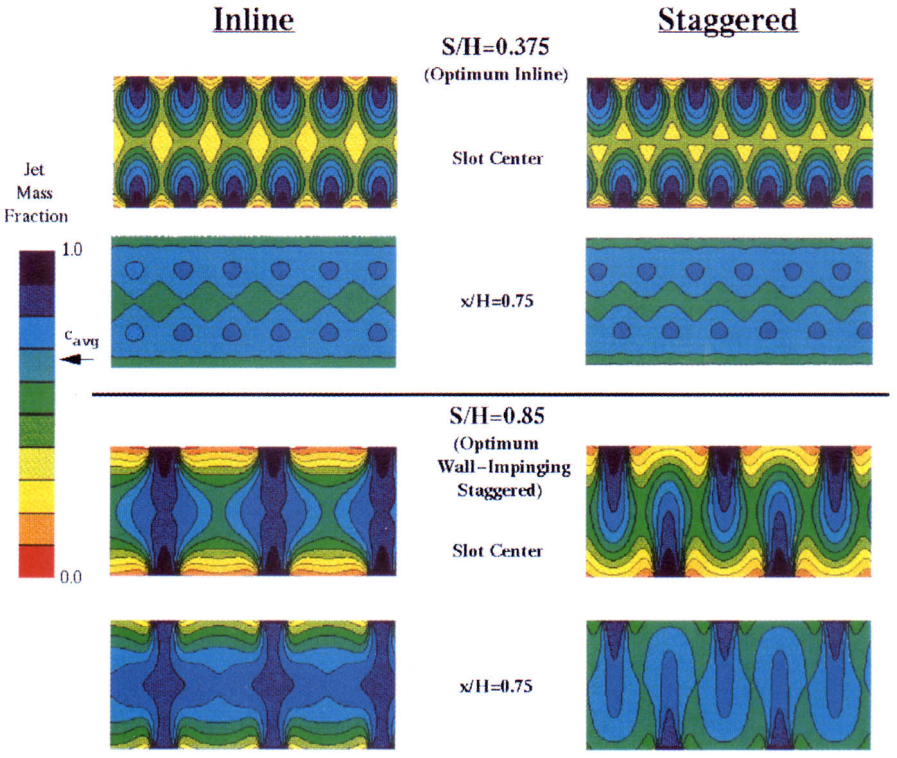

Fig. 13 Comparison of inline and wall-impinging staggered slots at optimum *S/H*: momentum-flux ratio 36, *MR* = 2.0.

terms, inline jets that penetrate to about one-fourth duct height produce optimum mixing.

Similar lateral slices showing jet penetration for staggered slots at *J* of 36 are shown in Fig. 5. The lateral planes in these figures are through the centerline of the top jets, and the corresponding plane through the bottom jet would be the reflected image of that shown. In contrast to optimum inline configurations, optimum staggered jets penetrate completely across the duct and impinge upon the opposite wall. As will be discussed later, another good mixing orifice spacing is obtained for staggered configurations if staggered jets are configured at optimum inline spacing. In this case, the staggered jets penetrate to one-fourth duct height, just like the optimum inline jets.

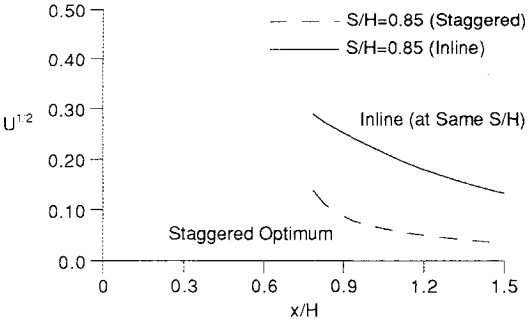

Fig. 14 Unmixedness comparison of inline and staggered configurations at staggered optimum *S/H*.

B. Effect of *J*

The effect of *J* on unmixedness is shown in Fig. 6 for inline slots, and in Fig. 7 for staggered slots. Each curve represents the optimum *S/H* for a specified *J*. Both lateral arrangements, staggered and inline, exhibited an initial mixing advantage gained by increasing *J* from 16 to 64. The improved initial mixing is caused by the slots being geometrically smaller as *J* increases from 16 to 64. Downstream mixing (i.e., *x/H* of 1.5) is seen to be similar for inline geometry as *J* varies, but substantial improvement is seen when *J* is increased for staggered configurations.

The jet mass fraction concentrations for inline and staggered slots are shown in Fig. 8. The location of the axial section is *x/H* of 0.75. Using the criteria of better mixing being indicated by fewer concentration levels, the cases for *J* of 64 are more thoroughly mixed than the *J* cases of 16 or 36. The enhancement in mixing by an increase in *J* is not unexpected due to a higher pressure drop experienced as *J* is increased.

C. Effect of Lateral Arrangement on Mixing

The effect of lateral arrangement on unmixedness is shown in Figs. 9, 10, and 11 for *J* of 16, 36, and 64, respectively. Only the curves corresponding to optimum *S/H* are presented. In each figure it can be seen that the inline slots have better initial mixing. This is due to the inline orifices being substantially smaller than staggered orifices. At locations farther downstream (i.e., *x/H* of 1.5), inline is better than staggered at *J* of 16, but inline is worse than staggered at *J* of 64. Indeed, the best mixing case of all cases studied is the staggered case shown in Fig. 11 for *J* for 64. The unmixedness values for the best mixing case was 0.02 at *x/H* of 1.5.

A more qualitative comparison of mixing illustrating the effect of lateral arrangement is presented in Fig. 12. This figure presents jet mass fraction color concentration maps for the optimum inline and staggered configurations at a momentum-flux ratio *J* of 36. The multiple cycles shown in this figure were generated graphically to maintain the same cross-sectional area for each case. It can be seen that the inline slots produce better initial mixing than the staggered slots at *x/H* of 0.75.

When experimental mixing tests are performed, only a limited number of orifice configurations can be tested. Typically, inline arrangements are first tested, followed by a lateral movement of one wall to produce staggered arrangements. If an inline arrangement at a given *J* is optimized (in terms of *S/H*), the corresponding staggered case obtained by laterally moving one wall will produce nearly identical mixing (see Fig. 13). The converse is not true; i.e., if a staggered arrangement at a given *J* is optimized, the corresponding inline case will produce inferior mixing (see Fig. 13).

Table 3 Empirically and numerically determined constants at optimum *S/H*

Geometry	Lateral arrangement	m_j/m_∞	J	S/H	$C = S/H \cdot \sqrt{J}$ Empirical	$C = S/H \cdot \sqrt{J}$ Numerical	Blockage %
Two-sided	Inline	2.0	16	—	1.25	2.0	35
↓	Inline	↓	36	—	↓	2.25	33
↓	Inline	↓	64	—	↓	2.28	33
↓	Staggered	↓	16	—	5.0	4.0	25
↓	Staggered	↓	36	—	↓	5.1	22
↓	Staggered	↓	64	—	↓	6.8	19

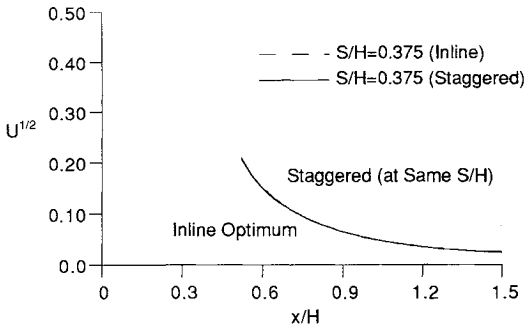

Fig. 15 Unmixedness comparison of inline and staggered configurations at inline optimum *S/H*.

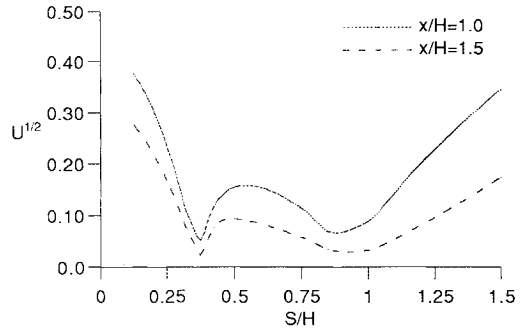

Fig. 16 Staggered cases produce double-valued function of unmixedness vs *S/H* (parametric 2, $J = 36$).

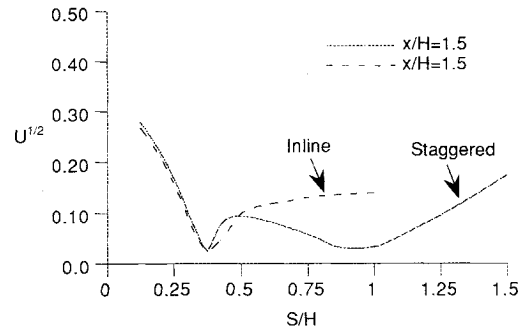

Fig. 17 Unmixedness comparison of inline and staggered slots for *S/H* variation at $x/H = 1.5$ ($J = 36$).

Figures 14 and 15 show the unmixedness comparisons of inline and staggered configurations at the same *S/H*. In Fig. 14 it is evident that running the inline configuration at optimum staggered spacing (*S/H* of 0.85) produces poorer mixing characteristics than the optimum staggered case. In contrast, there is no difference seen (see Fig. 15) between inline and staggered results at the optimum inline spacing (*S/H* of 0.375). Staggered configurations thus have two minimum values of unmixedness, as shown in Fig. 16 for *J* of 36. One minimum value corresponds to the optimum *S/H* arrangement for wall-impinging jets (*S/H* of 0.85), and the other minimum value corresponds to jets not being able to penetrate by each other (*S/H* of 0.375). Inline configurations have only a unique minimum unmixedness value (at *S/H* of 0.375) as shown in Fig. 17.

D. Comparison to Empirical Calculations for Optimum Mixing

Shown in Table 3 are the empirically and numerically determined constants for optimum mixing for the cases studied. For the inline cases, the numerical constant is about 75% higher than the empirical constant. Most of this difference may be attributed to the effect of mass-flow ratio, since the empirical constants were based on experiments with mass-flow ratios less than 0.50, while the numerical constants were determined with a mass-flow ratio of 2.0. (In other CFD studies not reported here, the numerical constant was only 30% higher than the empirical constant for a mass-flow ratio of 0.5.) Note that the jet blockage (at the wall) was about 33% for all *J* values. The constant blockage for all *J* values is expected due to geometry considerations if blockage is not important in the mixing process.

For the staggered cases, the numerical constants vary from 20% low for *J* of 16 to 36% high for *J* of 64. This agreement is considered adequate from an engineering design viewpoint, but there is probably a secondary effect (e.g., grid density, inlet turbulence boundary conditions, etc.) that is causing the disagreement.

VII. Conclusions

A CFD parametric mixing study was performed on axially opposed rows of staggered and inline jets injected into confined rectangular crossflow. The analysis was performed at *J* of 16, 36, and 64, *S/H* of 0.125–1.5, and a *MR* of 2.0. Based on the numerical results, the following conclusions can be drawn:

1) Inline configurations have better initial mixing than staggered configurations at their respective optimum *S/H*.

2) In terms of overall downstream mixing, (i.e., at *x/H* of 1.5), the optimum inline configuration is better than the optimum staggered configuration for *J* of 16, but the opposite is true for *J* of 64. Thus, the best configuration (in terms of inline or staggered) depends on *J*.

3) Increasing *J* improves initial mixing at optimum *S/H*. Increasing *J* improves downstream mixing (i.e., *x/H* of 1.5) for staggered configurations, but has negligible effect for inline configurations.

4) The optimum mixing equation $[(S/H)\sqrt{J} = C]$ of Holdeman[14] was found to be substantiated, except the constant *C* was increased by a factor of about 1.8 for two-sided inline configurations for jet-to-mainstream *MR*s of 2.0.

Acknowledgments

This work was supported by NASA Contract NAS3-25967, and NAS computer time was provided by NASA Lewis Research Center. Valuable discussions and assistance were provided by Milind Talpallikar.

References

[1]Shaw, R. J., "Engine Technology Challenges for a 21st Century High Speed Civil Transport," AIAA 10th International Symposium

on Air Breathing Engines, ISABE 93-7064, Sept. 1991; also NASA TM 104363, Sept. 1991.

[2]Mosier, S. A., and Pierce, R. M., "Advanced Combustion Systems for Stationary Gas Turbine Engines," Vol. I, Environmental Protection Agency Contract 68-02-2136, March 1980.

[3]Smith, C. E., "Mixing Characteristics of Dilution Jets in Small Gas Turbine Combustors," AIAA Paper 90-2728, July 1990.

[4]Smith, C. E., Talpallikar, M. V., and Holdeman, J. D., "A CFD Study of Jet Mixing in Reduced Flow Areas for Lower Combustor Emissions," AIAA Paper 91-2460, June 1991; also NASA TM 104411, June 1991.

[5]Vranos, A., Liscinsky, D. S., True, B., and Holdeman, J. D., "Experimental Study of Cross-Stream Mixing in a Cylindrical Duct," AIAA Paper 91-2459, June 1991; also NASA TM 105180, June 1991.

[6]Talpallikar, M. V., Smith, C. E., Lai, M. C., and Holdeman, J. D., "CFD Analysis of Jet Mixing in Low NO_x Flametube Combustors," *Journal of Engineering for Gas Turbines and Power*, Vol. 114, No. 2, 1992, pp. 416–424; also NASA TM 104466, April 1992.

[7]Hatch, M. S., Sowa, W. A., Samuelsen, G. S., and Holdeman, J. D., "Jet Mixing into a Heated Cross Flow in a Cylindrical Duct: Influence of Geometry and Flow Variances," AIAA Paper 92-0773, Jan. 1992; also NASA TM 105390, Jan. 1992.

[8]Bain, D. B., Smith, C. E., and Holdeman, J. D., "CFD Mixing Analysis of Jets Injected from Straight and Slanted Slots into Confined Crossflow in Rectangular Ducts," AIAA Paper 92-3087, July 1992; also NASA TM 105699, July 1992.

[9]Liscinsky, D. S., True, B., Vranos, A., and Holdeman, J. D., "Experimental Study of Cross-Stream Mixing in a Rectangular Duct," AIAA Paper 92-3090, July 1992; also NASA TM 106194, July 1992.

[10]Oechsle, V. L., Mongia, H. C., and Holdeman, J. D., "A Parametric Numerical Study of Mixing into a Cylindrical Duct," AIAA Paper 92-3088, July 1992; also NASA TM 105695, July 1992.

[11]Zhu, G., and Lai, M.-C., "A Parametric Study of Penetration and Mixing of Radial Jets in Necked-Down Cylindrical Crossflow," AIAA Paper 92-3091, July 1992.

[12]Kroll, J. T., Sowa, W. A., Samuelsen, G. S., and Holdeman, J. D., "Optimization of Circular Orifice Jets Mixing into a Heated Crossflow in a Cylindrical Duct," AIAA Paper 93-0249, Jan. 1993; also NASA TM 105984, Jan. 1993.

[13]Liscinsky, D. S., Vranos, A., and Lohmann, R. P., "Experimental Study of Crossflow Mixing in Cylindrical and Rectangular Ducts," NASA CR 187141, March 1993.

[14]Holdeman, J. D., "Mixing of Multiple Jets with a Confined Subsonic Crossflow," *Progress in Energy and Combustion Sciences*, Vol. 19, June 1993; also AIAA Paper 91-2458, 1991; NASA TM 104412, 1991.

[15]Przekwas, A. J., Habchi, S. D., Yang, H. Q., Avva, R. K., Talpallikar, M. V., and Krishnan, A., "REFLEQS-3D: A Computer Program for Turbulent Flows with and Without Chemical Reaction, Volume 1: User's Manual," CFD Research Corp. Rept. GR-89-4, Huntsville, AL, Jan. 1990.

[16]Danckwertz, P. V., "The Definition and Measurement of Some Characteristics of Mixtures," *Applied Scientific Research*, Sec. A, Vol. 3, 1952, pp. 279–296.

Color reproductions courtesy of NASA Lewis Research Center